Controlling femtosecond filament propagation using externally-driven gas motion

J. K. WAHLSTRAND,[1,2] **N. J**HAJJ,[1] AND **H. M. M**ILCHBERG[1,*]

[1]*Institute for Research in Electronics and Applied Physics, University of Maryland, College Park, MD 20742, USA*
[2]*Currently with Physical Measurement Laboratory, National Institute of Standards and Technology, Gaithersburg, MD 20899, USA*
*Corresponding author: milch@umd.edu

The thermal density depression (or "density hole") produced by a high repetition rate femtosecond filament in air acts as a negative lens, altering the propagation of the filament. We demonstrate the effects of externally driven gas motion on these density holes and the resulting filament steering, and we derive an expression for the gas velocity that maximizes the effect. At gas velocities more than ~3 times this value, the density hole is displaced from the filament and no longer affects filament propagation. We demonstrate density hole displacement using an audio speaker-driven sound wave, leading to a controllable, repeatable deflection of the filament. Applications are discussed, including quasi phase matching in gas-based nonlinear optics. To our knowledge, this is the first demonstration of femtosecond filament propagation control through controlled motion of the nonlinear medium.

When an intense ultrashort optical pulse propagates through transparent media, the interplay of diffraction, self-focusing, and plasma defocusing can result in propagation of a high intensity core portion of the beam (typically of width ~50-100 μm) over many Rayleigh lengths without appreciable intensity reduction [1]. This phenomenon has been called 'femtosecond filamentation'. The high intensity and long interaction length can enable self-compression [2–4] and high harmonic generation [5–7]. In air, the propagating pulse deposits energy through plasma generation and molecular rotation of nitrogen and oxygen [8,9]. This energy deposition thermalizes and eventually dissipates, first by acoustic wave emission after an acoustic timescale $\tau_a \sim a/c_s \sim$100-300 ns, where a is the filament core radius and ~3×10^4 cm/s is the sound speed in ambient air, followed by thermal diffusion. At the time of acoustic wave emission, $t \sim \tau_a$, a density depression (or 'density hole') of peak depth of up to ~30% of ambient density and maximum peak temperature change $\Delta T \sim$ 100 K begins to broaden and decrease by thermal diffusion over several milliseconds, a timescale set by the thermal diffusivity of air. During this phase of the evolution, the density hole is in pressure balance with the ambient gas. The result is an extended and long-lived channel of decreased gas density [10-12]. This extended density hole plays a role in potential applications such as triggering of electrical discharges [10,11] and is central to our development of long-lived air waveguides [13,14].

If the repetition rate of a train of filament-forming pulses is high enough (>~200 Hz in air), each pulse propagates through the cumulative density hole left behind by the filaments generated by the preceding pulses. The density hole acts as an effective negative lens, altering the propagation of the filaments [12,15]. In Ref. [15] it was shown that upward motion of the heated gas due to buoyancy leads to deformation of the cumulative density hole and a downward deflection of the laser beam, without appreciable change in the mode quality. Any motion of the gas in which the cumulative density hole is embedded can cause beam steering. For example, we have found that a 1 kHz repetition rate filament in air propagating along the axis of a metal tube, installed to block laboratory air currents, is extremely sensitive to vibrations of the tube. We attribute this to the coupling of tube vibrations to motion of the air inside the tube.

The density hole can be viewed as a transducer, coupling the movement of air to optical propagation. While the sensitivity of the beam pointing to small gas flows could be deleterious for some applications of filament-induced density holes, it also suggests avenues of control. In this paper, we discuss the effects of gas motion on high repetition rate filaments in air. We first present a simple model based on the effect of air heating by a femtosecond filament on propagation of a subsequent filament. This gives a lower bound on the beam deflection effect. We then simulate the effect of the cumulative density hole produced by a high repetition rate femtosecond filament in the presence of a steady state gas flow. Experimental results are then presented demonstrating controlled beam deflection using a loudspeaker-driven acoustic wave. These are compared to numerical simulations.

At the typical peak intensity of 10^{13}-10^{14} W/cm² and pulse duration <100 fs of a filamenting optical pulse, energy is deposited in air by field ionization (plasma generation) and two-photon rotational excitation (molecular rotation) [16,17] as discussed earlier. With respect to the hydrodynamic and thermal timescales of air, this deposition is an impulse excitation [12] because the electron-neutral collision time (<0.5 ps), the electron-ion recombination timescale (~1 ns) and the thermalization time of the excited rotational population (~100 ps) [18] are all much less than the acoustic timescale τ_a. Therefore one can assume, as the initial condition for driving the hydrodynamic and thermal response of the air, that the filament's impulse deposition of energy is entirely repartitioned into the thermal degrees of freedom of neutral air [12]. Our previous work has measured and simulated the air acoustic and thermal dynamics of single filaments and arrays of filaments [19], and this assumption is well supported.

Here, we are mainly interested in the thermal portion of the dynamics at times $t > \tau_a$, where the density hole, starting from its maximum depth and peak temperature, decays by thermal diffusion. Throughout this process, the density hole is in pressure balance with the ambient air. The cross sectional temperature profile during diffusive relaxation of an approximately axially (z) invariant section of density hole is well modeled by $T(x,y,t) = T_a + \Delta T(t) \exp[-(x^2+y^2)/R^2(t)]$, where $\Delta T(t) = \Delta T_{peak} R_0^2/R^2(t)$, $R(t) = (R_0^2 + 4\alpha t)^{1/2}$, R_0 is the $1/e$ radius of the initial Gaussian temperature distribution with peak temperature change ΔT_{peak}, T_a is ambient air temperature, and $\alpha = 0.19$ cm^2/s is the thermal diffusivity of air [20]. For the energy deposition of typical single filaments, $\Delta T_{peak} \sim 50\text{-}100$ K [12,13]. As the air is in pressure equilibrium during this phase of the evolution, the change in density is given by $\Delta N/N_a \approx -\Delta T/T_a$, where N_a is the ambient gas density.

The density changes affect the propagation of light through the dependence of the refractive index on density. The change in index at time delay t for a single pulse is

$$\Delta n_{\text{single}}(t) = (n_0 - 1)\frac{\Delta N}{N_a}$$
$$\approx -(n_0 - 1)\frac{\Delta T_{\text{peak}}}{T_a}\frac{R_0^2}{R^2(t)}e^{-\frac{x^2+y^2}{R^2(t)}}, \tag{1}$$

where n_0 is the ambient refractive index. In air at $T_a = 300$ K, $N_a = 2.5\times10^{19}$ cm^{-3}, and $n_0-1 = 2.8\times10^{-4}$, an initial density drop at $t \sim \tau_a$ of ~30% consistent with $\Delta T_{peak} \sim 100$ K gives $\Delta n \sim 5\times10^{-7}$ after 1 ms, enough to measurably affect propagation of a 1 kHz filament [12,15].

At high repetition rates the thermally induced change in density due to many pulses accumulates, deepens, and deviates from a pure Gaussian shape [12,15]. Consider a train of pulses indexed by m starting at 0. For small temperature changes, the density changes due to each pulse can simply be added, so that the cumulative index change just before the arrival of pulse m is $\Delta n \approx \sum_{i=1}^{m} \Delta n_{single}(i\Delta t)$, where Δt is the interval between pulses. For $\Delta t \gg R_0^2/4\alpha$, we find $\Delta n \approx -\sum_{i=1}^{m}(n_0 - 1)(\Delta T_{peak}/T_a)(R_0^2/4\alpha i\Delta t)$. This harmonic sum is approximately $\Delta n \approx -(n_0 - 1)\left(\frac{\Delta T_{peak}}{T_a}\right)\left(\frac{R_0^2}{4\alpha\Delta t}\right)[\gamma + \ln(m)]$, where $\gamma \approx 0.577$ is the Euler-Mascheroni constant. The divergence of this expression for large m would seem to indicate that the temperature of the gas in the filament core rises without limit as the pulse train continues depositing energy in the gas. In a real gas, however, neglected effects such as convective gas motion limit the temperature rise.

If the deepest point of the density hole is not centered on the laser beam, the filament will propagate through a refractive index gradient, causing it to deflect. This has been measured and modeled in our prior work, where the center mismatch is caused by buoyancy of the density hole, with local upward motion of the air [15]. In this paper, we are interested in the effect of *externally driven* air motion on the filament. Filament deflection can be estimated using a ray propagation model [15]. For a weak deflection angle $\Delta\theta < R(\Delta t)/L$, where L is the filament length, a reasonable approximation is that a ray sees the same refractive index gradient as it passes through the region containing the density depression. The deflection angle is then proportional to the distance D that the beam propagates through the region of refractive index gradient. Returning to the assumption that only the effect of the immediately preceding pulse matters, we find using Eq. (1), for a Gaussian density depression centered at $(x,y) = (x_0,0)$ and a ray launched at $(x,y) = (0,0)$, that the deflection angle per unit propagation distance along the optical axis (z) is given by

$$\frac{\Delta\theta}{D} = \int \frac{d\Delta n(x(z),z)}{dx}dz$$
$$\approx -(n_0 - 1)\frac{\Delta T_{\text{peak}}}{T_a}\frac{2x_0 R_0^2}{R^4(t)}e^{-x_0^2/R^2(t)}. \tag{2}$$

The deflection angle $\Delta\theta/D$ is maximized for $x_0 = R(t)/\sqrt{2}$. If the density hole is generated in a steady gas flow of velocity u, it is displaced by $x_0 = u\Delta t$ in a time interval Δt. Therefore, the velocity u_{defl} at which a subsequent pulse delayed by Δt is maximally deflected is $u_{\text{defl}} = R(t+\Delta t)/(\sqrt{2}\,\Delta t)$. In air, for an initial Gaussian density profile full-width-at-half-maximum (FWHM) of $2R_{1/2} = 2(\ln2)^{1/2} R_0 \sim 50$ μm, $\Delta T_{\text{peak}} = 50$ K, and $\Delta t = 1$ ms (for a 1 kHz laser), $u_{\text{defl}} = 0.2$ m/s and $\Delta\theta/D = 1.5$ mrad/m of propagation.

The non-Gaussian density profile produced by pulse train heating of a gas moving at constant flow velocity u is simulated by numerically solving the heat flow equation $\partial T/\partial t = -\alpha\nabla^2 T$, assuming a sequence of pulses, indexed by m starting at 0, and separated by $\Delta t = 1$ ms. The entering laser beam is centered on $(x,y)=(0,0)$. Pulse $m = 1$ first samples the density hole, which has moved a distance $\Delta x = u\Delta t$ after initial generation. Each pulse changes the temperature profile by $\delta T(x,y)$, giving a cumulative temperature profile change of $\Delta T(x,y)$. The result is an asymmetric accumulation of heating [15]. Figures 1a and 1b show the density hole profile $\Delta N(x,y) \approx -N_a \Delta T(x,y)/T_a$ seen by pulse m for flow velocities $u = 0.1$ m/s and $u = 0.3$ m/s. Since the density hole acts as a negative lens, the filament deflects in the direction opposite to the translation of the density hole [15].

The effect of the accumulated energy deposition and air heating on successive pulses can be studied by examining the evolution of the deflection with pulse number, as calculated using Eq. (2) and shown in Fig. 1c. The deflection increases with pulse number until a steady state is reached, with steady state reached faster with higher flow velocity. The dependence of beam deflection on flow velocity is shown in Fig. 1d for various pulses m in the pulse train. For pulse $m = 1$, the deflection is maximized for $u = u_{\text{defl,max}} = 0.2$ m/s, consistent with the prediction of Eq. (2). For later pulses ($m = 5, 9, 14$), the deflection is maximized at lower flow velocity, while at high velocities all curves asymptotically approach the prediction of Eq. (2), which includes only the effect of the previous pulse in the train. This is because the gas is moving so rapidly that the temperature rise from previous pulses has been swept away. At sufficiently high flow velocity, the density hole produced by pulse m is displaced by more than its width so that pulse $m+1$ encounters nearly unperturbed gas. From Fig. 1d, it is seen that this occurs for flow velocities $> \sim 3u_{\text{defl,max}}$. Therefore, for high repetition rate laser pulses, one can avoid the effects of a cumulative density hole with a sufficiently rapid gas flow.
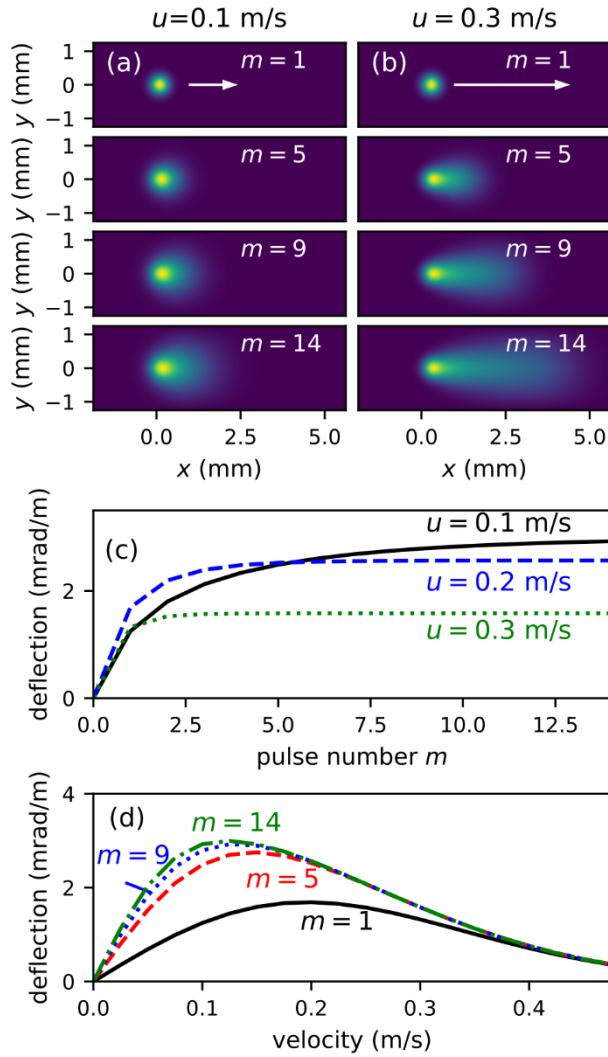
Fig. 1. Simulations of the gas density profile produced by a 1 kHz filament in air versus steady state gas velocity u and pulse number m, showing the development of the asymmetric density distribution: (a) u = 0.1 m/s; (b) u = 0.3 m/s. (c) Beam deflection as a function of pulse number for u = 0.1 m/s (solid black), u = 0.2 m/s (dashed blue), and u = 0.3 m/s (dotted green). (d) Beam deflection as a function of flow velocity for m = 1 (solid black), 5 (dashed red), 9 (dotted blue), and 14 (dash-dotted green).

Controllable, rapidly changing gas velocity distributions can be generated with acoustic waves. Consider a monochromatic sound wave of frequency Ω, with $f=\Omega/2\pi < \sim 1$ kHz. For air sound speed of c_s = 340 m/s, this corresponds to acoustic wavelength $\lambda_a=c_s/f>\sim 30$ cm, much larger than the width of the cumulative density hole, which is millimeters at most. Thus, a filament produced in such an acoustic field would encounter air with a locally uniform density and an oscillating flow velocity. Acoustic amplitude is ordinarily given in decibels as A_s = $20\log_{10}(P_{\mathrm{rms}}/P_{\mathrm{ref}})$, where P_{rms} is the root mean squared pressure amplitude and P_{ref} is a reference level, 20 µPa in air [21]. The peak mean particle velocity v ($\sim u$) is related to P_{rms} by $v=2^{1/2}P_{\mathrm{rms}}/Z$, where Z = 410 Pa·s/m is the acoustic impedance in air at standard atmospheric conditions [21]. The

maximum gas displacement $\Delta x=u/f$. To produce a displacement of order of the density hole width after 1 ms, $\Delta x \sim$ 300 µm, an acoustic level of 101 dB is required at f = 25 Hz.

A diagram of the experiment is shown in Fig. 2. Pulses of energy 2.4 mJ, pulse width 50 fs, and wavelength 800 nm from a 1 kHz Ti:Sapphire amplifier were focused in air with a 1 m lens at f/250 to generate a $\sim$30 cm long filament, as estimated by the extent of the plasma fluorescence. Based on observation of the far field mode profile, the beam propagated as a single filament. A speaker (30 cm diameter subwoofer) was placed 25 mm below the filament's most intense region. The beam pointing in the far field was measured using a quadrant detector [15]. The signal from the detector was calibrated so that the beam deflection could be found in mrad. The speaker was driven by a sinusoidal waveform at 25 Hz. We measured the acoustic output of the speaker with a microphone and found it to be free of harmonic distortion for all amplitudes used in the experiment. We did not have a way of relating the peak current amplitude driving the speaker to the maximum velocity. However, based on the observed motion of the speaker in its linear regime, (up to <1 cm peak-to-peak) and the driving frequency, we can place an upper bound of 0.75 m/s on the peak velocity. This is consistent with our simulations, as discussed later.
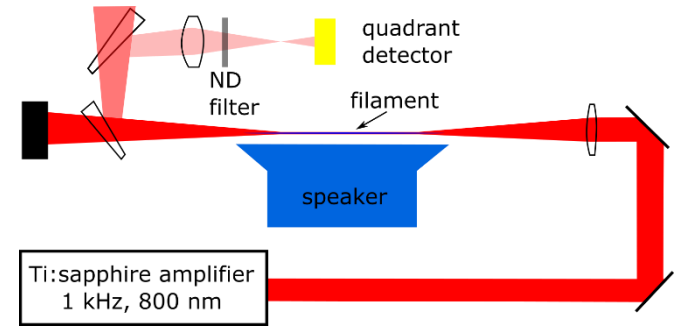

Fig. 2. Experimental diagram. The femtosecond filament propagates over a speaker, and the beam deflection is measured using a quadrant photodiode downstream.

The left side of Fig. 3 shows the measured deflection of the beam as a function of time. At the lowest driving amplitude (0.5 A peak input current) as shown in the top left panel, the deflection is roughly sinusoidal and oscillates at 25 Hz. In this case, we expect the maximum driven flow velocity to be less than $\sim u_{\mathrm{defl,max}}$. At higher driving current amplitudes (middle and bottom panels), the deflection undergoes a more rapid, hard saturation at $\sim$1.0 mrad and rebounds, as seen in the increasing 'cupping' at the curve peaks. We attribute this to the fluid velocity in the sound wave exceeding several times $u_{\mathrm{defl,max}}$. Under these conditions, the speaker-induced air motion translates the density hole increasingly out of the path of successive femtosecond filaments, thus reducing the measured deflection. The maximum deflection amplitude of <0.25 mrad is consistent with our earlier estimates given a filament length of $\sim$0.3m. The right side of Fig. 3 shows simulations of the beam deflection as a function of time in a sinusoidally oscillating gas flow (for peak gas velocity 0.02, 0.15, and 0.35 m/s) using the first line of Eq. (2) to find the beam deflection from the temperature distribution calculated using the heat equation, assuming an initial temperature rise of 50 K and a 30 cm filament. The simulation assumed axially uniform heating

over the full filament length and an axially uniform translation of the gas by the speaker. We find excellent agreement, except for an asymmetry in the experimental data. We speculate that this is caused by a small DC air flow, produced either by buoyant motion of the heated gas [15] or air currents in the laboratory.
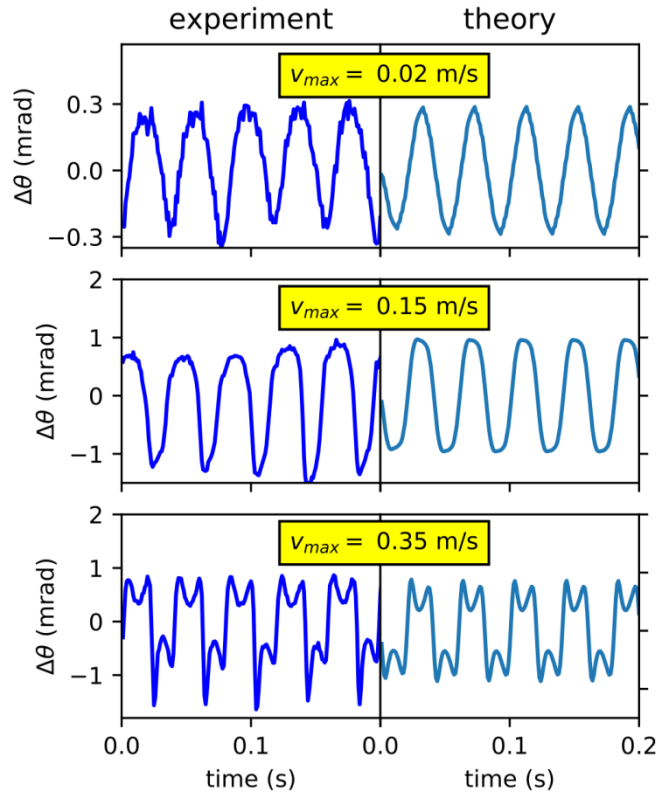

Fig. 3. Experimental results (left) for three speaker current amplitudes, from top to bottom: 0.5 A, 0.9 A, and 2.4 A. Simulations (right) of the beam deflection using Eq. (2) and the heat conduction equation, assuming an initial temperature rise of 50 K and a 30 cm filament, for peak gas velocity 0.02, 0.15, and 0.35 m/s.

In summary, we have explored the steering of high repetition rate femtosecond filaments by externally-driven gas flows, demonstrating acoustically-driven beam deflection. Control of beam pointing is one potential application, but there are other promising applications. Quasi phase matching in gas-based nonlinear optics has been used for high harmonic generation, based on modulated hollow core glass waveguides [22]. Sapaev *et al.* theoretically considered direct production of density modulations using an acoustic wave [23]. This requires very high intensity, high frequency sound. By combining lower frequency, lower amplitude sound with filament-produced density depressions, it would be possible to create density modulations an order of magnitude higher than can be easily produced by sound alone. A modulation of the sound amplitude could be produced in an acoustic cavity, or simply by placing a mask between a speaker and the filament in the near (acoustic) field. Use of this effect could enable quasi phase matching of high harmonics at high repetition rates in the filamentary or sub-filamentary intensity regime.

References

1. A. Couairon and A Mysyrowicz, Phys. Rep. **441**, 47–189 (2007).
2. C. P. Hauri, W. Kornelis, F. W. Helbing, A. Heinrich, A. Couairon, A. Mysyrowicz, J. Biegert, and U. Keller, Appl. Phys. B **79**, 673–7 (2004).
3. G. Stibenz, N. Zhavoronkov, and G. Steinmeyer, Opt. Lett. **31**, 274–6 (2006).
4. D. S. Steingrube, M. Kretschmar, D. Hoff, E. Schulz, T. Binhammer, P. Hansinger, G. G. Paulus, U. Morgner, and M. Kovacev, Opt. Express **20**, 24049–58 (2012).
5. Y. Tamaki, J. Itatani, Y. Nagata, M. Obara, and K. Midorikawa, Phys. Rev. Lett. **82**, 1422–5 (1999).
6. J. C. Painter, M. Adams, N. Brimhall, E. Christensen, G. Giraud, N. Powers, M. Turner, M. Ware, and J. Peatross, Opt. Lett. **31**, 3471–3 (2006).
7. T. Popmintchev, M.-C. Chen, D. Popmintchev, P. Arpin, S. Brown, S. Ališauskas, G. Andriukaitis, T. Balčiunas, O. D. Mücke, A. Pugzlys, A. Baltuška, B. Shim, S. E. Schrauth, A. Gaeta, C. Hernández-García, L. Plaja, A. Becker, A. Jaron-Becker, M. M. Murnane, and H. C. Kapteyn, Science **336**, 1287–91 (2012).
8. E. W. Rosenthal, N. Jhajj, I. Larkin, S. Zahedpour, J. K. Wahlstrand, and H. M. Milchberg, Opt. Lett. **41**, 3908 (2016).
9. E. W. Rosenthal, J. P. Palastro, N. Jhajj, S. Zahedpour, J.K. Wahlstrand, and H.M. Milchberg, J. Phys. B **48**, 094011 (2015).
10. F. Vidal, D. Comtois, C.-Y. Chien, A. Desparois, B. La Fontaine, T. W. Johnston, J. Kieffer, H. P. Mercure, H. Pepin and F. A. Rizk, IEEE Trans. Plasma Sci. **28**, 418–33 (2000).
11. S. Tzortzakis, B. Prade, M. Franco, A. Mysyrowicz, S. Hüller, and P. Mora, Phys. Rev. E **64**, 057401 (2001).
12. Y.-H. Cheng, J. K. Wahlstrand, N. Jhajj, and H. M. Milchberg, Opt. Express **21**, 4740–51 (2013).
13. N. Jhajj, E. W. Rosenthal, R. Birnbaum, J. K. Wahlstrand, and H. M. Milchberg, Phys. Rev. X **4**, 011027 (2014).
14. E. W. Rosenthal, N. Jhajj, J. K. Wahlstrand, and H. M. Milchberg, Optica **1**, 5 (2014).
15. N. Jhajj, Y.-H. Cheng, J. K. Wahlstrand, and H. M. Milchberg, Opt. Express **21**, 28980–6 (2013).
16. D. V. Kartashov, A. V. Kirsanov, A. M. Kiselev, A. N. Stepanov, N. N. Bochkarev, Y. N. Ponomarev, and B. A. Tikhomirov, Opt. Express **14**, 7552–8 (2006).
17. S. Zahedpour, J. K. Wahlstrand, and H. M. Milchberg, Phys. Rev. Lett. **112**, 143601 (2014).
18. Y.-H. Chen, S. Varma, A. York, and H. M. Milchberg, Opt. Express **15**, 11341 (2007).
19. J. K. Wahlstrand, N. Jhajj, E. W. Rosenthal, S. Zahedpour, and H. M. Milchberg, Opt. Lett. **39**, 1290-1293 (2014).
20. "Thermophysical Properties of Air," in CRC Handbook of Chemistry and Physics, 99th Edition (Internet Version 2018), John R. Rumble, ed., CRC Press/Taylor & Francis, Boca Raton, FL.
21. Lawrence Kinsler, Austin Frey, Alan Coppens, and James Sanders, *Fundamentals of Acoustics*. New York: John Wiley & Sons, Inc. (2000).
22. I. P. Christov, H. C. Kapteyn, and M. M. Murnane, Opt. Express **7**, 362-367 (2000).
23. U. K. Sapaev, I. Babushkin, and J. Herrmann, Opt. Express **20**, 22753-22762 (2012).

References with titles

1. A. Couairon and A Mysyrowicz, "Femtosecond filamentation in transparent media," Phys. Rep. **441**, 47–189 (2007).

2. C. P. Hauri, W. Kornelis, F. W. Helbing, A. Heinrich, A. Couairon, A. Mysyrowicz, J. Biegert and U. Keller, "Generation of intense, carrier-envelope phase-locked few-cycle laser pulses through filamentation," Appl. Phys. B **79**, 673–7 (2004).

3. G. Stibenz, N. Zhavoronkov, and G. Steinmeyer, "Self-compression of millijoule pulses to 7.8 fs duration in a white-light filament," Opt. Lett. **31**, 274–6 (2006).

4. D. S. Steingrube, M. Kretschmar, D. Hoff, E. Schulz, T. Binhammer, P. Hansinger, G. G. Paulus, U. Morgner, and M. Kovacev, "Sub-1.5-cycle pulses from a single filament," Opt. Express **20**, 24049–58 (2012).

5. Y. Tamaki, J. Itatani, Y. Nagata, M. Obara, and K. Midorikawa, "Highly Efficient, Phase-Matched High-Harmonic Generation by a Self-Guided Laser Beam," Phys. Rev. Lett. **82**, 1422–5 (1999).

6. J. C. Painter, M. Adams, N. Brimhall, E. Christensen, G. Giraud, N. Powers, M. Turner, M. Ware, and J. Peatross, "Direct observation of laser filamentation in high-order harmonic generation," Opt. Lett. **31**, 3471–3 (2006).

7. T. Popmintchev, M.-C. Chen, D. Popmintchev, P. Arpin, S. Brown, S. Ališauskas, G. Andriukaitis, T. Balčiunas, O. D. Mücke, A. Pugzlys, A. Baltuška, B. Shim, S. E. Schrauth, A. Gaeta, C. Hernández-García, L. Plaja, A. Becker, A. Jaron-Becker, M. M. Murnane, and H. C. Kapteyn, "Bright Coherent Ultrahigh Harmonics in the keV X-ray Regime from Mid-Infrared Femtosecond Lasers," Science **336**, 1287–91 (2012).

8. E. W. Rosenthal, N. Jhajj, I. Larkin, S. Zahedpour, J. K. Wahlstrand, and H. M. Milchberg, "Energy deposition of single femtosecond filaments in the atmosphere," Opt. Lett. **41**, 3908 (2016).

9. E. W. Rosenthal, J. P. Palastro, N. Jhajj, S. Zahedpour, J.K. Wahlstrand, and H.M. Milchberg, "Sensitivity of propagation and energy deposition in femtosecond filamentation to the nonlinear refractive index," J. Phys. B **48**, 094011 (2015).

10. F. Vidal, D. Comtois, C.-Y. Chien, A. Desparois, B. La Fontaine, T. W. Johnston, J. Kieffer, H. P. Mercure, H. Pepin and F. A. Rizk, "Modeling the triggering of streamers in air by ultrashort laser pulses," IEEE Trans. Plasma Sci. **28**, 418–33 (2000).

11. S. Tzortzakis, B. Prade, M. Franco, A. Mysyrowicz, S. Hüller, and P. Mora, "Femtosecond laser-guided electric discharge in air," Phys. Rev. E **64**, 057401 (2001).

12. Y.-H. Cheng, J. K. Wahlstrand, N. Jhajj, and H. M. Milchberg "The effect of long timescale gas dynamics on femtosecond filamentation," Opt. Express **21**, 4740–51 (2013).

13. N. Jhajj, E. W. Rosenthal, R. Birnbaum, J. K. Wahlstrand, and H. M. Milchberg, "Demonstration of Long-Lived High-Power Optical Waveguides in Air," Phys. Rev. X **4**, 011027 (2014).

14. E. W. Rosenthal, N. Jhajj, J. K. Wahlstrand, and H. M. Milchberg, "Collection of remote optical signals by air waveguides," Optica **1**, 5 (2014).

15. N. Jhajj, Y.-H. Cheng, J. K. Wahlstrand, and H. M. Milchberg, "Optical beam dynamics in a gas repetitively heated by femtosecond filaments," Opt. Express **21**, 28980–6 (2013).

16. D. V. Kartashov, A. V. Kirsanov, A. M. Kiselev, A. N. Stepanov, N. N. Bochkarev, Y. N. Ponomarev, and B. A. Tikhomirov, "Nonlinear absorption of intense femtosecond laser radiation in air," Opt. Express **14**, 7552–8 (2006).

17. S. Zahedpour, J. K. Wahlstrand, and H. M. Milchberg, "Quantum Control of Molecular Gas Hydrodynamics," Phys. Rev. Lett. **112**, 143601 (2014).

18. Y.-H. Chen, S. Varma, A. York, and H. M. Milchberg, "Single-shot, space- and time-resolved measurement of rotational wavepacket revivals in H_2, D_2, N_2, O_2, and N_2O," Opt. Express **15**, 11341 (2007).

19. J. K. Wahlstrand, N. Jhajj, E. W. Rosenthal, S. Zahedpour, and H. M. Milchberg, "Direct imaging of the acoustic waves generated by femtosecond filaments in air," Opt. Lett. **39**, 1290-1293 (2014).

20. "Thermophysical Properties of Air," in CRC Handbook of Chemistry and Physics, 99th Edition (Internet Version 2018), John R. Rumble, ed., CRC Press/Taylor & Francis, Boca Raton, FL.

21. Lawrence Kinsler, Austin Frey, Alan Coppens, and James Sanders, *Fundamentals of Acoustics*. New York: John Wiley & Sons, Inc. (2000).

22. I. P. Christov, H. C. Kapteyn, and M. M. Murnane, "Quasi-phase matching of high-harmonics and attosecond pulses in modulated waveguides," Opt. Express **7**, 362-367 (2000).

23. U. K. Sapaev, I. Babushkin, and J. Herrmann, "Quasi-phase-matching for third harmonic generation in noble gases employing ultrasound," Opt. Express **20**, 22753-22762 (2012).